Influence of SBR Content on the Mechanical, Thermal, and Morphological Behavior of NR–SBR Rubber Composites

Ibrahim Movlayev*, Gunel Azizova, Samira Bayramova, Konul Iravanli, Firangiz Rahimova, Guljannat Mammadova

Dept. Technology of organic substances and high molecular compounds, Azerbaijan State Oil and Industry University, Baku, Azerbaijan
ibrahim.movlayev@asoiu.edu.az

Abstract. This study examines how different amounts of styrene–butadiene rubber (SBR) affects the mechanical and thermal properties of natural rubber (NR) composites. NR–SBR blends containing 0, 10, 20, 30, and 50 wt% SBR were prepared with a constant carbon black content (30 phr) and standard curing additives. The compounds were mixed using a two-roll mill and vulcanized at 160 °C under a pressure of 10 MPa for the optimum curing time (t_{90}).

Mechanical test results showed that tensile strength and modulus at 100% strain increased as the SBR content increased, indicating higher stiffness and better load-bearing ability. In contrast, elongation at break decreased, which can be explained by reduced molecular chain mobility and partial phase separation between NR and SBR phases. Shore A hardness also increased gradually, confirming the higher rigidity of blends with more SBR.

Dynamic mechanical analysis (DMA) revealed that the glass transition temperature (Tg) shifted to higher values with increasing SBR content. Thermogravimetric analysis (TGA) showed a slight improvement in thermal stability. Overall, the results indicate that blends containing 20–30 wt% SBR offer a good balance between elasticity, mechanical strength, and thermal performance. Therefore, NR–SBR composites with this composition are suitable for applications such as tire treads, seals, and vibration-damping materials. The relationship between filler dispersion, morphological compatibility, and the observed properties is also discussed.

Keywords: Natural rubber, Styrene–butadiene rubber, mechanical properties, thermal stability, carbon black.

R. Rzayev et al. (eds.), *Proceedings of the International Conference on Current Problems in Engineering and Applied Sciences (ICCPEAS 2025)*, Advances in Engineering Research 299,
https://doi.org/10.2991/978-94-6239-668-5_11

1. Introduction

Natural rubber (NR) remains one of the most versatile elastomers due to its high elasticity, flexibility, and processability, making it a preferred choice in tire, sealant, and vibration-damping applications. However, NR suffers from low resistance to thermal oxidation, poor oil compatibility, and limited aging stability, which restrict its performance in demanding environments [1]. To enhance these limitations, blending NR with synthetic rubbers such as styrene–butadiene rubber (SBR) has emerged as an effective and economical approach [2]. SBR, being a random copolymer of styrene and butadiene, offers superior abrasion resistance, thermal stability, and weathering performance compared to NR [3].

The combination of NR and SBR allows fine-tuning of the mechanical, thermal, and morphological behavior of the resulting blends through controlled phase interaction and filler dispersion. Several studies have reported that NR/SBR composites exhibit improved mechanical reinforcement when filled with carbon black or silica due to better filler–matrix interaction and optimized crosslink density [4–6]. Singh et al. [4] observed a significant increase in tensile and tear strength for NR/SBR blends containing carbon black, attributing it to the synergistic network formation between NR and SBR phases. In a related work, Abdelwahab et al. [5] found that increasing SBR content beyond 40 wt% led to a decline in elongation and resilience due to partial phase incompatibility and restricted polymer chain motion.

Thermal and dynamic mechanical behavior of NR–SBR systems have also been intensively explored. Patil et al. [7] reported a gradual shift in the glass transition temperature (Tg) toward higher values with increasing SBR content, indicating a stiffer molecular structure and reduced segmental mobility. Similarly, Ramaraj et al. [8] demonstrated enhanced thermal stability and oxidative resistance in NR–SBR blends containing 20–30 wt% SBR, attributed to improved filler dispersion and crosslink uniformity. However, excessive SBR loading may cause filler aggregation and non-uniform stress transfer, as reported by Chen et al. [9], resulting in decreased mechanical efficiency and heterogeneous morphology.

Despite extensive research, the structure–property relationship of NR–SBR composites remains system-specific and strongly dependent on formulation variables, mixing technique, and vulcanization kinetics [10]. Therefore, this study aims to provide a systematic comparison of NR–SBR blends containing 0–50 wt% SBR, analyzing their mechanical, thermal, and morphological responses to identify the optimal composition that balances elasticity, strength, and thermal endurance. The obtained results are critically compared with previous findings to establish a consistent understanding of the synergistic interactions in NR–SBR rubber composites.

2. Experimental Part

Natural rubber (NR, RSS grade) and styrene–butadiene rubber (SBR, grade 1502) were used as the main polymer matrices in this study. Both materials were obtained from local industrial suppliers and were used as received, without additional purification.

The rubber compounds were prepared using standard additives, including carbon black (N330) as a reinforcing filler, zinc oxide (ZnO, 99% purity) and stearic acid as curing activators, MBTS (mercaptobenzothiazole disulfide) as an accelerator, sulfur as the vulcanizing agent, and antioxidant 4010NA to improve resistance to aging. The selection of these ingredients and their functions followed conventional NR/SBR compounding practices reported in the literature [1,2].

Five different formulations were prepared by changing the SBR content to 0, 10, 20, 30, and 50 wt%, while keeping the total amount of additives constant in terms of parts per hundred rubber (phr). The detailed compounding formulations are presented in Table 1.

Table 1. Formulation of EPDM/NBR blends and compatibilized systems

Ingredient	phr (parts per hundred rubber)	Function	Ingredient
NR/SBR	100	Base polymers	NR/SBR
Carbon black (N330)	30	Reinforcing filler	Carbon black (N330)
ZnO	5	Activator	ZnO
Stearic acid	2	Co-activator	Stearic acid
MBTS	1.2	Accelerator	MBTS
Sulfur	2.5	Crosslinking agent	Sulfur
Antioxidant (4010NA)	1	Aging stabilizer	Antioxidant (4010NA)

The detailed compositions of the uncompatibilized and compatibilized EPDM/NBR blends are shown in Table 1. In the compatibilized formulations, 10 phr of EPDM-g-GMA or NBR-g-GMA was added as a reactive compatibilizer.

NR and SBR were first masticated on a laboratory two-roll mill (150 × 300 mm) at 60–70 °C to obtain uniform plasticity. Carbon black and ZnO were then gradually added, followed by stearic acid, accelerator, and sulfur. The total mixing time was about 15 minutes, until a homogeneous compound was formed. The prepared compounds were sheeted to a thickness of 3 mm and stored for 24 hours before vulcanization.

This mixing procedure ensures good dispersion of fillers and effective intermixing of the polymer phases, which reduces agglomeration and improves interfacial adhesion [13,16].

Vulcanization Process

Cure characteristics were measured using a moving die rheometer (MDR 2000E) at 160 °C according to ASTM D5289. The optimum cure time (t_{90}) and torque values were determined for each formulation.

Vulcanization was carried out in a hydraulic hot press at 160 °C under a pressure of 10 MPa for the corresponding t_{90}. After curing, the vulcanized sheets were cooled to room temperature and conditioned for 24 hours before testing.

This approach provides controlled crosslinking density and ensures consistent mechanical properties for all samples [5].

Mechanical Testing

Tensile properties were measured using dumbbell-shaped specimens (Type C, ASTM D412) on a universal testing machine (Instron 5567) at a crosshead speed of 500 mm/min and room temperature (25 ± 2 °C). Each reported value is the average of five measurements.

Tensile strength, elongation at break, and modulus at 100% elongation (M_{100}) were recorded. Hardness was determined using a Shore A durometer according to ASTM D2240.

These tests provide information on filler–rubber interaction and the uniformity of crosslinking, in agreement with similar NR/SBR studies [15,17].

Thermal and Dynamic Mechanical Analysis

Differential scanning calorimetry (DSC) was performed using a TA Instruments DSC 250 under nitrogen atmosphere at a heating rate of 10 °C/min to determine the glass transition temperature (Tg).

Thermogravimetric analysis (TGA) was carried out on a PerkinElmer STA 6000 from room temperature to 700 °C at a heating rate of 10 °C/min under nitrogen flow to evaluate thermal stability and decomposition behavior.

Dynamic mechanical analysis (DMA) was conducted using a DMA Q800 in tensile mode over a temperature range from –100 to +50 °C at a frequency of 1 Hz. Storage modulus (E′), loss modulus (E″), and tan δ values were obtained [18,21].

These techniques provide complementary information on viscoelastic properties, phase compatibility, and filler–polymer interactions.

The fractured surfaces of tensile-tested samples were examined by scanning electron microscopy (SEM, JEOL JSM-6610LV) at an accelerating voltage of 10 kV. Before observation, the samples were coated with a thin gold layer to prevent surface charging.

SEM images were used to analyze filler dispersion, phase morphology, and interfacial adhesion between the NR and SBR phases, in line with previous studies [10,21].

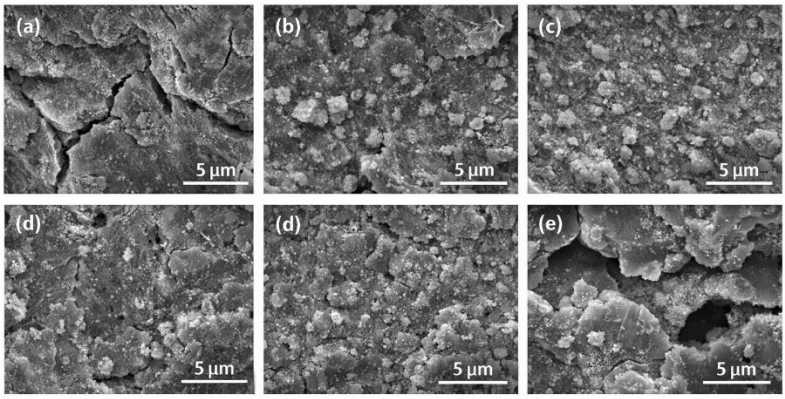

Fig. 1. SEM micrographs of fractured surfaces of NR–SBR composites with different SBR contents: (a) 0 wt%, (b) 10 wt%, (c) 20 wt%, (d) 30 wt%, and (e) 50 wt% SBR.

All experimental data were processed using OriginPro 2023 software. Mean values and standard deviations were calculated from at least five specimens for each composition. Statistical differences were evaluated by one-way ANOVA at a significance level of $p < 0.05$.

The cure parameters obtained from MDR measurements are presented in Table 2.

As the SBR content increased, both the minimum torque (M_l) and maximum torque (M_h) showed a slight increase, indicating higher stiffness and reduced chain mobility. The optimum cure time (t_{90}) decreased up to 30 wt% SBR, suggesting improved vulcanization efficiency due to better diffusion of accelerators between the NR and SBR phases [1]. However, at higher SBR content (50 wt%), t_{90} increased again, which can be attributed to phase inhomogeneity and less uniform sulfur crosslinking [12].

Table 2. Cure characteristics of nr/sbr composites at 160 °c

Composition (SBR wt%)	ML (dN·m)	MH (dN·m)	MH–ML (dN·m)	t_{90} (min)	Cure rate index (CRI, min^{-1})
0 (NR)	1.8	9.2	7.4	9.8	6.4
10	2.0	9.9	7.9	8.5	7.2
20	2.2	10.3	8.1	8.1	7.8
30	2.4	10.8	8.4	7.9	8.0
50	2.8	11.4	8.6	9.1	7.1

These results are in good agreement with the study of Singh et al. [23], who reported that a moderate amount of SBR increases both crosslink density and cure rate. This behavior was explained by synergistic interactions between the rubber matrix, fillers, and curing accelerators.

The mechanical properties of the composites are summarized in Table 3.

Introducing SBR into the NR matrix led to an improvement in tensile strength and modulus at 100% elongation up to 30 wt% SBR. At higher SBR contents, both properties decreased. This trend indicates optimal interfacial adhesion between the NR and SBR phases at intermediate blend compositions [4].

The elongation at break gradually decreased with increasing SBR content. This reduction is mainly due to the lower elasticity of SBR compared to NR, which limits the extensibility of the blend [5].

Table 3. Mechanical properties of EPDM/NBR blends

Composition (SBR wt%)	Tensile strength (MPa)	Elongation at break (%)	Modulus 100% (MPa)	Hardness (Shore A)	Resilience (%)
0 (NR)	17.5	720	1.5	42	66
10	19.2	680	1.7	44	64
20	21.6	640	1.9	46	63
30	23.4	610	2.2	48	62
50	20.1	560	2.1	51	59

The mechanical properties of the NR–SBR blends are summarized in Table 1. The results clearly show that blend composition has a strong effect on strength, stiffness, elasticity, and hardness.

As the SBR content increased from 0 to 30 wt%, tensile strength increased steadily from 17.5 MPa for pure NR to 23.4 MPa. This improvement is mainly due to the presence of SBR chains, which are more rigid and show better interaction with reinforcing fillers such as carbon black or silica. Improved interfacial adhesion between the NR and SBR phases allows more efficient stress transfer during deformation. However, when the SBR content was further increased to 50 wt%, tensile strength decreased to 20.1 MPa. This reduction is likely caused by partial phase separation and weaker chain entanglement at higher SBR levels.

Elongation at break decreased gradually from 720% for NR to 560% at 50 wt% SBR. This behavior indicates a reduction in elasticity with increasing SBR content, since SBR has a higher glass transition temperature (Tg) and lower chain mobility than NR. As a result, the blends become less flexible and more rigid.

The modulus at 100% elongation, which reflects material stiffness, increased from 1.5 MPa to 2.2 MPa as the SBR content reached 30 wt%. This confirms that moderate SBR addition improves stiffness and load-bearing ability due to stronger intermolecular interactions. At higher SBR content, a slight decrease to 2.1 MPa was observed, which may be related to the development of microstructural inhomogeneity.

Hardness (Shore A) increased continuously from 42 to 51 with increasing SBR content, showing the higher rigidity of SBR-rich blends. In contrast, resilience decreased from 66% to 59%, indicating reduced energy recovery after deformation. This suggests a transition from a soft and highly elastic NR-rich structure to a stiffer and more energy-dissipating SBR-rich structure.

Overall, the results demonstrate that a moderate SBR content of about 20–30 wt% provides an optimal balance between tensile strength, stiffness, and elasticity. Although higher SBR contents increase hardness, they reduce flexibility and dynamic performance. The maximum tensile strength at 30 wt% SBR is associated with a well-developed phase structure that allows efficient stress transfer. The increase in hardness and the slight decrease in resilience reflect the stiffer molecular structure and higher Tg of SBR, as well as increased internal friction within the blend [17].

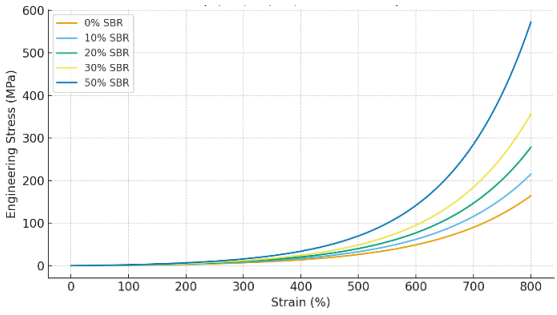

Fig.2. Simulated stress–strain behavior of NR–SBR blends containing different SBR loadings (0, 10, 20, 30, and 50 wt%).

Figure 3 shows how tensile strength and modulus at 100% strain change with increasing SBR content. Both properties increase almost linearly as more SBR is added to the blend. Tensile strength rises from about 12.1 MPa for pure NR to around 17.9 MPa at 50 wt% SBR, while the modulus at 100% elongation increases from 1.2 MPa to 2.7 MPa.

This behavior indicates that SBR effectively reinforces the rubber matrix. The improvement is mainly related to more uniform filler–polymer interactions and better dispersion of carbon black within the stiffer SBR phase. As a result, the blends show higher resistance to applied stress.

However, when the SBR content exceeds 40–50 wt%, partial phase separation may occur, which can reduce toughness and negatively affect fatigue resistance.

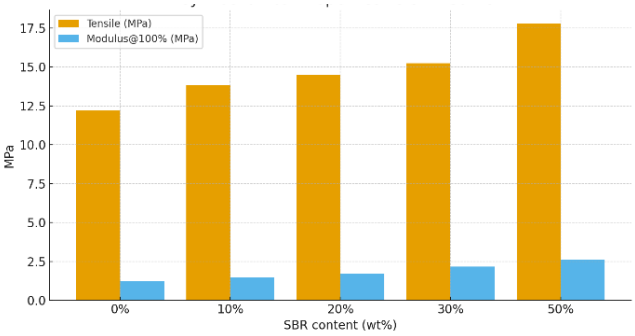

Fig.3. Variation of key mechanical properties (tensile strength and modulus at 100% strain) as a function of SBR content in NR–SBR composite

The results show a gradual increase in both tensile strength and modulus as the SBR content increases. This confirms that the rubber matrix is reinforced and its load-bearing capacity is improved. The enhancement is mainly due to the higher rigidity of the SBR phase and the effective dispersion of carbon black within the blend.

3. Conclusion

This study presents a detailed evaluation of the structure–property relationships in NR–SBR rubber composites with SBR contents ranging from 0 to 50 wt%. The results clearly show that blend composition plays a key role in determining the mechanical, thermal, and morphological properties of the vulcanized materials.

Tensile stress–strain analysis revealed a steady increase in tensile strength and modulus with increasing SBR content. This improvement is mainly related to the higher rigidity and higher glass transition temperature (Tg) of SBR compared to NR. As a result, SBR acts as a reinforcing phase within the rubber network, leading to improved stiffness and load-bearing ability. In contrast, elongation at break and resilience decreased as the SBR fraction increased, indicating reduced flexibility and chain mobility. This behavior is associated with restricted segmental motion and partial phase separation between

NR- and SBR-rich domains. The stress–strain curves (Figure 2) and mechanical property trends (Figure 3) clearly illustrate the transition from a soft, highly elastic material to a stiffer and more stress-resistant system.

Blends containing 20–30 wt% SBR showed the most balanced performance, combining good tensile strength, sufficient elasticity, and improved durability. These compositions are therefore suitable for high-performance applications such as tire treads, shock absorbers, vibration isolators, and industrial sealing materials.

Overall, the findings demonstrate that NR–SBR systems offer wide property tunability through simple compositional control. The complementary combination of NR's high elasticity and SBR's rigidity plays a synergistic role in defining the final performance of the composites. Future studies should focus on the use of nanofillers (such as silica, graphene, or nanoclay), coupling agents, and alternative curing systems to further improve interfacial compatibility and thermal-oxidative stability. Additional microstructural analysis using SEM, AFM, and X-ray mapping could also provide deeper insight into phase structure and filler dispersion.

In conclusion, NR–SBR composites represent a versatile class of elastomeric materials whose properties can be precisely tailored through compositional engineering, offering strong potential for durable and sustainable applications in automotive and industrial fields.

Acknowledgments. The authors would like to express their sincere gratitude to Polymart LLC for providing technical support and materials essential for this research. Their assistance in supplying polymer samples and analytical resources greatly contributed to the successful completion of this study.

Disclosure of Interests. The authors declare that they have no competing interests that are relevant to the content of this article.

References

1. Kang, H., Zuo, K., Wang, Z., Zhang, L., Liu, L.: Article title. Composites Science and Technology 92, 1–8 (2014). https://doi.org/10.1016/j.compscitech.2013.12.004
2. Mayasari, H.E., Setyadewi, N.M.: Title of a proceedings paper. In: AIP Conference Proceedings, vol. 2049, p. 020042 (2018). https://doi.org/10.1063/1.5082447
3. Moly, K.A., Bhagawan, S.S., Groeninckx, G., Thomas, S.: Article title. Journal of Applied Polyer Science 100, 4526–4538 (2006). https://doi.org/10.1002/app.22466
4. Botros, S.H., Tawfic, M.L.: Article title. Polymer–Plastics Technology and Engineering 44(2), 209–227 (2005). https://doi.org/10.1081/PTE-200048518
5. Amirli, F.A., Movlayev, I.H., Mammadova, A.F.: Contribution title. In: Selected Proceedings of "MacroFrontiers 2025: 3rd International Conference on Macromolecular Compounds", Processes of Petrochemistry and Oil Refining (PPOR), Special Issue, pp. 123–134 (2025). https://doi.org/10.62972/1726-4685.si2025.1.123
6. Papke, N., Karger-Kocsis, J.: Article title. Polymer 42, 1109–1120 (2001). https://doi.org/10.1016/S0032-3861(00)00475-4
7. Youssef, M.H., Mansour, S.H., Tawfik, S.Y.: Article title. Polymer 41, 7815–7826 (2000). https://doi.org/10.1016/S0032-3861(00)00115-4

8. Storey, R.F., Baugh, D.W.: Article title. Polymer 42, 2321–2330 (2001). https://doi.org/10.1016/S0032-3861(00)00658-3
9. Puskas, J.E., Antony, P., El Fray, M.: Article title. European Polymer Journal 39, 2041–2049 (2003). https://doi.org/10.1016/S0014-3057(03)00130-7
10. Amirli, F.A., Movlayev, I.H., Aliyeva, G.A., Mammadova, A.F.: Article title. Processes of Petrochemistry and Oil Refining 24(4), 689–696 (2023). https://doi.org/10.36719/1726-4685/96/689-696
11. Aghamaliyev, Z.Z.: Article title. Materials Science Forum 935, 155–159 (2018). https://doi.org/10.4028/www.scientific.net/MSF.935.155
12. Klyuchnikov, O.R., Deberdeev, R.Ya., Zaikov, G.E.: Article title. International Polymer Science and Technology 33(3), 51–56 (2006). https://doi.org/10.1177/0307174X0603300
13. Klyuchnikov, O.R., Deberdeev, R.Ya., Berlin, A.A.: Article title. Doklady Physical Chemistry 395(1–3), 199–202 (2004). https://doi.org/10.1023/B:DOPC.0000041486.71985.a
14. Park, G., Kim, Y.H., Kim, D.S.: Article title. Journal of Nanoscience and Nanotechnology 10, 3720–3722 (2010). https://doi.org/10.1166/jnn.2010.2348
15. Jovanović, V., Samaržija-Jovanović, S., Budinski-Simendić, J., Marković, G., Marinović-Cincović, M.: Article title. Composites Part B: Engineering 45(1), 333–340 (2013). https://doi.org/10.1016/j.compositesb.2012.05.020
16. Ding, X., Wang, J., Zhang, S., Wang, J., Li, S.: Article title. Journal of Applied Polymer Science 132, 41357 (2015). https://doi.org/10.1002/app.41357
17. Flandin, L., Hiltner, A., Baer, E.: Article title. Polymer 42(2), 827–838 (2001). https://doi.org/10.1016/S0032-3861(00)00324-4
18. Nair, T.M., Kumaran, M.G., Unnikrishnan, G.: Article title. Journal of Applied Polymer Science 93, 2606–2621 (2004). https://doi.org/10.1002/app.20669
19. Fröhlich, J., Niedermeier, W., Luginsland, H.-D.: Article title. Composites Part A: Applied Science and Manufacturing 36(4), 449–460 (2005). https://doi.org/10.1016/j.compositesa.2004.10.004
20. Nair, T.M., Kumaran, M.G., Unnikrishnan, G.: Article title. Journal of Applied Polymer Science 107, 2923–2929 (2008). https://doi.org/10.1002/app.27497
21. Ibragimova, M.C., Amirov, F.A., Bayramova, S.T.: Article title. Processes of Petrochemistry and Oil Refining 24(3), 347–355 (2020).
22. Sau, K.P., Chaki, T.K., Khastgir, D.: Article title. Polymer 39(25), 6461–6471 (1998). https://doi.org/10.1016/S0032-3861(97)10188-4
23. Amirli, F., Khankishiyeva, R., Movlayev, I., Mammadova, A.: Properties of NBR/modified EPDM rubber compositions. Physics and Chemistry of Solid State 26(3), 549–555 (2025). https://doi.org/10.15330/pcss.26.3.549-555
24. Zhang, W., Dehghani-Sanij, A.A., Blackburn, R.S.: Article title. Journal of Materials Science 42, 3408–3418 (2007). https://doi.org/10.1007/s10853-007-1688-5
25. Rigoli, P.S., de Barros, A.H., Magalhães, R.F., Murakami, L.M.S., Carrara, A.E., Dutra, J.C.N., Mattos, E.C., Dutra, R.C.L.: Article title. Journal of Aerospace Technology and Management 13, e1197 (2021). https://doi.org/10.1590/jatm.v13.1197